

UNCLASSIFIED
AD 430091

DEFENSE DOCUMENTATION CENTER

FOR

SCIENTIFIC AND TECHNICAL INFORMATION

CAMERON STATION, ALEXANDRIA, VIRGINIA



UNCLASSIFIED

NOTICE: When government or other drawings, specifications or other data are used for any purpose other than in connection with a definitely related government procurement operation, the U. S. Government thereby incurs no responsibility, nor any obligation whatsoever; and the fact that the Government may have formulated, furnished, or in any way supplied the said drawings, specifications, or other data is not to be regarded by implication or otherwise as in any manner licensing the holder or any other person or corporation, or conveying any rights or permission to manufacture, use or sell any patented invention that may in any way be related thereto.

430091

CATALOGED BY DDC

430091

AS AC 13.



AN EXPERIMENTAL INVESTIGATION
OF FLUTTER OF A FULLY SUBMERGED
SUBCAVITATING HYDROFOIL

BY

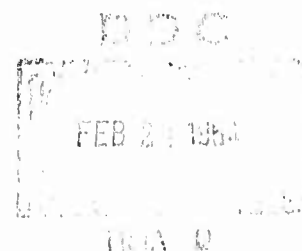
H. NORMAN ABRAMSON
GUIDO E. RANSLEBEN, JR.

TECHNICAL REPORT NO. 4
CONTRACT NO. NONR - 3335(00)
SWRI PROJECT NO. 38-1028-2

PREPARED FOR

DEPARTMENT OF THE NAVY
BUREAU OF SHIPS HYDROFOIL PROGRAM
SUBPROJECT SS 600 000
ADMINISTERED BY THE DAVID TAYLOR MODEL BASIN
WASHINGTON 25, D.C.

15 DECEMBER 1963



SOUTHWEST RESEARCH INSTITUTE
SAN ANTONIO HOUSTON

SOUTHWEST RESEARCH INSTITUTE
8500 Culebra Road, San Antonio, Texas 78206

Department of Mechanical Sciences

AN EXPERIMENTAL INVESTIGATION
OF FLUTTER OF A FULLY SUBMERGED
SUBCAVITATING HYDROFOIL

by

H. Norman Abramson
Guido E. Ransleben, Jr.

Technical Report No. 4
Contract No. Nonr-3335(00)
SwRI Project No. 38-1028-2

Prepared for

Department of the Navy
Bureau of Ships Hydrofoil Program
Subproject SS 600 000
Administered by the David Taylor Model Basin
Washington 25, D. C.

15 December 1963

APPROVED:

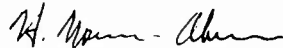

H. Norman Abramson, Director
Department of Mechanical Sciences

TABLE OF CONTENTS

	<u>Page</u>
List of Tables	ii
List of Figures	iii
ABSTRACT	iv
INTRODUCTION	1
EXPERIMENTAL PROGRAM	1
Description of Flutter Model	1
Model Suspension and Excitation System	3
Instrumentation and Test Procedures	5
Catastrophic Failure	5
ANALYSIS	6
DISCUSSION	8
Acknowledgements	11
References	12

LIST OF TABLES

<u>Table</u>		<u>Page</u>
I	Flutter Model Design Parameters	13
II	Oscillatory Hydrodynamic Coefficients for $1/k = 0$	14
III	Oscillatory Hydrodynamic Coefficients for $1/k = .500$	14
IV	Oscillatory Hydrodynamic Coefficients for $1/k = .700$	15
V	Oscillatory Hydrodynamic Coefficients for $1/k = .833$	15
VI	Oscillatory Hydrodynamic Coefficients for $1/k = .900$	16
VII	Oscillatory Hydrodynamic Coefficients for $1/k = 1.00$	16
VIII	Oscillatory Hydrodynamic Coefficients for $1/k = 1.10$	17
IX	Oscillatory Hydrodynamic Coefficients for $1/k = 1.25$	17
X	Oscillatory Hydrodynamic Coefficients for $1/k = 1.67$	18

LIST OF FIGURES

<u>Figure</u>		<u>Page</u>
1	Schematic Layout of Flutter Model and Suspension	19
2	Details of Flutter Model Construction	20
3	Flutter Model Following Catastrophic Failure at 48.1 knots	21
4	Flutter Model Impaled in Towing Carriage Wall Following Catastrophic Failure	22
5	Flutter Model Exponential Decay Factor Versus Speed	23
6	Coupled Torsional Frequency Versus Speed	24

ABSTRACT

This paper presents the results of an investigation of the flutter characteristics of a fully submerged subcavitating hydrofoil. The foil suffered a catastrophic flutter failure at a speed of approximately 48 knots. Comparisons are made with various prediction methods, neither the two-dimensional nor the three-dimensional theoretical calculations yielding results of the correct order of magnitude. Calculations employing measured three-dimensional oscillatory coefficients give a highly conservative prediction for flutter speed.

INTRODUCTION

The possible occurrence of classical bending-torsion flutter of a fully submerged subcavitating hydrofoil has been questioned repeatedly over the past several years. In the absence of definitive and authoritative evidence of such a flutter occurrence, or related experimental data, opinions have ranged from the impossibility of flutter to speculation as to the inapplicability of conventional aerodynamic flutter theory.¹ As part of a fundamental experimental investigation into these questions, the authors have conducted a series of tests with special hydrofoil models capable of providing directly the three-dimensional coefficients of oscillatory lift and moment due to cantilever wing bending and torsion, in water. This data covers a range of low values of reduced velocity and has been presented in detail elsewhere.^{2,3} A bending-torsion flutter model was also constructed and tested as part of this research program, and it is the presentation of data regarding this flutter model to which the present paper is directed.

EXPERIMENTAL PROGRAM

Description of Flutter Model

The hydrofoil flutter model (Fig. 1) was deliberately

designed to be flutter prone, in order to provide a definite experimental point for correlation with various analytical predictions.

A mass ratio ($\mu = \frac{m}{\pi \rho b^2}$) of unity was arbitrarily selected for the model as being small enough to demonstrate behavior in the range of interest to hydrofoil applications, but large enough to insure that flutter would occur. This mass ratio is also about as large a value as can be practically achieved with a 12% thick foil section of solid lead. An NACA 16-012 airfoil section was chosen in order to have the center of gravity near midchord. The elastic axis was located well ahead of the c. g., and the bending and torsional stiffnesses were held low in order to obtain a low flutter speed. Further, in order to simplify and enhance the accuracy of the analytical procedures, the model parameters were made uniform spanwise and the spar, being the only continuous spanwise member, provided a well defined elastic axis.

The remaining model design parameters were also chosen on the basis of values that would result in the lowest practicable flutter speed, as given in Table I. The actual values of these various parameters, as determined by measurements from the model, are also shown. While the uncoupled bending frequency was found to be close to the design value, the torsional frequency was approximately twice as large as the design value, primarily

as the result of failing to account properly for the stiffening effects of the spar attachments.

The model was composed of isolated spanwise strips connected by a single H-beam spar. The spar was machined from 4340 steel and was designed to have a high chordwise bending stiffness as compared with the lateral bending and torsional stiffness. The foil contour was formed by cast lead sections with embedded steel webs to provide additional rigidity. The webs were first welded to steel blocks, which then were allowed to project from the lead castings to provide for mounting to the spar caps. A typical section is shown in Figure 2. Each lead section was approximately 1.90 inches wide, separated from the adjacent section by a gap of approximately 0.10 inch and sealed with Silastic RTV 731 approximately 0.10 inch thick. The foil contour was filled out over the spar caps with a lead-filled plastic poured in place and trimmed to contour. This material was of such composition that it would hold its shape, but without contributing significantly to the spar stiffness. A stainless steel plate was employed to close the tip of the model.

Model Suspension and Excitation System

The spar extended past the model root and fittings were attached for mating with the same support fairing used for the load-measuring models employed earlier.³ The root end was therefore

held rigidly so that the model was cantilevered vertically from the towing carriage (Fig. 1).

An internal system for dynamic excitation of the model was desired in order that no disturbance to the fluid flow would result. This system consisted simply of two 7/16 in. diameter rods passing through the spar on each side of the web (Fig. 2) and anchored to the model tip, but free floating along the rest of the span and extending through the model root and up to the upper side of the carriage frame. Crank arms connected with links were attached to the upper ends of the rods and a cable attached to the end of these cranks extended to the sides of the towing carriage. When the cable was suddenly pulled, the torque applied to the rods twisted the model tip slightly. The rods were also designed to serve as components of a brake system to prevent structural damage to the model should a violent mode of flutter be encountered. For this purpose, the cranks at the top ends of the rods could be clamped between two manually operated levers to increase the overall torsional stiffness of the model.*

* Because the torsional stiffness of the model was actually much higher than originally anticipated, the added stiffness provided by the clamped rods was not significant and thus the braking system was rendered ineffective.

Instrumentation and Test Procedures

Instrumentation consisted of two strain gage bridges on the spar root, one being sensitive to spar bending and one to spar torsion. Signals from these bridges were recorded on an oscillograph and, additionally, the torsion signal was also displayed on an oscilloscope. A high-speed motion picture camera was stationed at a single point along the length of the towing basin. All tests were conducted on the high speed carriage at the David Taylor Model Basin.

The towing carriage speed was varied in increments of approximately 5 knots, from an initial speed of 10 knots. As soon as a given speed was established, the recording oscillograph was started and the exciting cable pulled, so that logarithmic decrements of the signal decay from the two strain gage bridges were thereby recorded. The decay of the torsion signal was simultaneously observed on the oscilloscope (Polaroid photo) and the logarithmic decrement obtained immediately. Thus, it was possible to maintain a continuing surveillance of the system damping as carriage speed increased. Some of the records taken at the higher carriage speeds were repeated.

Catastrophic Failure

At a carriage speed of approximately 45 knots, the measured

logarithmic decrement showed a significant decrease in damping and therefore the next speed increment was selected to be only 2-1/2 knots. However, the actual carriage speed was 48.1 knots, resulting in a strong flutter condition growing from the initial disturbance applied to the model and leading to catastrophic failure of the model within a few seconds. Structural failure occurred at the spar root, as shown in Figure 3. The model then slid off of the exciter rods (which were bent to an angle of about 90°), rose completely out of the water, and impaled itself in the rear wall (1/8 in. aluminum sheet) of the test bay of the carriage (Fig. 4).

The flutter frequency was approximately 17.5 cps, resulting in a value of reduced velocity at flutter of $(V/b\omega)_F = 1.48$. By a rather fortuitous circumstance, the oscillatory motion of the foil had just attained rather large amplitudes as it passed the point at which the motion picture camera was stationed so that a short film record was obtained. The film shows some cavitation arising from these large amplitude motions, just prior to the structural failure.

ANALYSIS

Three flutter analyses have been performed in order to compare various prediction methods with the measured flutter

speed of this model. The various analyses are all based on a ten-station strip theory Rayleigh-type calculation⁴, and differ from each other only in the values employed for the oscillatory lift and moment coefficients.

One analysis was made employing conventional two-dimensional theoretical coefficients⁴ and one was made employing modified three-dimensional theoretical coefficients;⁵ the third analysis employed the measured three-dimensional coefficients³. The measured three-dimensional coefficients were originally obtained in terms of moment about the 31% chord position. The more conventional quarter-chord coefficients are then obtained from the relations

$$\begin{aligned} L_h &= L_{hh} \\ L_\alpha &= L_{h\alpha} \\ M_h &= M_{\alpha h} + m_b/b L_{hh} \\ M_\alpha &= M_{\alpha\alpha} + m_t/b L_{hh} \end{aligned}$$

where $m_b/b = 0.1131$ for the bending model and $m_t/b = 0.1108$ for the torsion model. The elastic axis was located at the quarter-chord position in both models. Values of the quarter-chord coefficients for the ten spanwise stations and nine nominal values of reduced velocity are given in Tables II-X, as interpolated from the actual experimental values.

The results of the various flutter analyses, together with the relevant experimental data* discussed earlier in this paper, are presented in Figure 5 in terms of the exponential decay factor (δ) versus speed (V). Points at which these curves intercept the speed axis are defined as critical flutter speeds.

Another comparison between the various analyses and the experimental data is shown in Figure 6 in terms of the coupled torsional frequency versus speed. The calculated values employing theoretical three-dimensional coefficients appear to give a trend most closely approximating that of the experimental data.

DISCUSSION

The results given in Figure 5 are striking in their differences. The two-dimensional theory predicts no critical speed at all while the three-dimensional theory leads to a critical speed that is unconservative by more than 100%. The calculation employing measured three-dimensional coefficients, on the other hand, predicts a flutter speed that is conservative by a substantial amount. Obviously, none of these can be considered a satisfactory

* The multiple experimental points at certain values of speed show the scatter of values of logarithmic decrement obtained for different test runs at that speed.

prediction of critical flutter speed.

Based on previous aeronautical experience with similar techniques,⁶ it would normally be expected that the calculation of flutter speed employing measured three-dimensional coefficients would yield a value in very close agreement with the measured flutter speed. As was pointed out in Reference 3, however, the measured coefficients employed here are known to be somewhat low in magnitude, particularly the moments, due to attenuation of response of the measuring system to loads aft of midchord, with an unknown effect on phase angles. This, coupled with some uncertainties in data reduction due to impure modes and high noise levels lends some doubt as to the ability to predict accurate flutter speeds with these measured coefficients.

Another factor which may warrant consideration resides in the observation of some partial cavitation occurring on the model during the large amplitude oscillations just preceding structural failure. There is, however, no evidence that this cavitation occurred before large amplitudes were built up.

Perhaps one more observation may be pertinent to this discussion. During the course of these calculations, some small changes in the numerical values of the various coefficients were

made with very large effects on the value of the critical flutter speed.* At least, one should conclude that, for the model parameters involved here, the critical flutter speed is extremely sensitive to the values of the oscillatory coefficients.

The results of analytical predictions of flutter speeds of fully submerged subcavitating hydrofoils should be viewed with skepticism, and substantiating evidence from model tests should be obtained whenever possible.

* These studies, aimed at developing a semi-empirical flutter prediction technique more generally valid than the conventional calculations reported here, are continuing.

ACKNOWLEDGEMENTS

The authors are grateful to Mr. Luis R. Garza and Mr. Willis L. Mynatt for invaluable assistance in the model construction and experimental program, and to Mr. Carl G. Langner and Mr. Robert Gonzales for performing the flutter calculations. Mr. David A. Jewell of DTMB gave generously of his support throughout this program.

REFERENCES

1. Abramson, H. Norman and Chu, Wen-Hwa, "A Discussion of the Flutter of Submerged Hydrofoils," Journal of Ship Research, 3, 2, pp. 5-13, October 1959.
2. Abramson, H. Norman and Ransleben, Guido E., Jr., "Experimental Unsteady Airfoil Lift and Moment Coefficients for Low Values of Reduced Velocity," AIAA Journal, 1, 6, pp. 1441-1443, June 1963.
3. Ransleben, Guido E., Jr. and Abramson H. Norman, "Experimental Determination of Oscillatory Lift and Moment Distributions on Fully Submerged Flexible Hydrofoils," Journal of Ship Research, 7, 2, pp. 24-41, October 1963.
4. Scanlan, Robert H. and Rosenbaum, Robert, AIRCRAFT VIBRATION AND FLUTTER, The Macmillan Company, New York, 1951.
5. Reissner, E. and Stevens, J. E., "Effect of Finite Span on the Airload Distributions for Oscillating Wings. II--Methods of Calculation and Examples of Application," NACA Technical Note 1195 (October 1947).
6. Epperson, T. B., Pengelley, C. D., Ransleben, G. E. Jr., Wilson, L. E., and Younger, D. G. Jr., "Nonstationary Airload Distributions on a Straight Flexible Wing Oscillating in a Subsonic Wind Stream," WADC Technical Report 55-323, U. S. Air Force, January 1956.

TABLE I. FLUTTER MODEL DESIGN PARAMETERS

<u>Model Design Parameters</u>	<u>Design Value</u>	<u>Actual Value</u>
Aspect ratio, R	5.00	5.00
Semichord, b	0.50 ft.	0.50 ft.
Mass ratio, μ	1.00	0.99
Elastic axis location, a	-0.50	-0.50
Center of gravity location, x_α	0.50	0.524
Radius of gyration, r_α^2	0.50	0.512
Bending stiffness, EI	$3.08 \times 10^6 \text{ lb-in}^2$	$3.40 \times 10^6 \text{ lb-in}^2$
Torsional stiffness, GJ	$0.311 \times 10^6 \text{ lb-in}^2$	$0.973 \times 10^6 \text{ lb-in}^2$
Frequency ratio, ω_h/ω_α	1.00	0.490
Torsion frequency, ω_α	10.0 cps*	20.5 cps*
Total weight	--	121.2 lb.

* Uncoupled natural frequencies in air

TABLE II. OSCILLATORY HYDRODYNAMIC COEFFICIENTS FOR $1/k = 0$

% Span	L_h		L_α		M_h		M_α	
	Mag.	Phase	Mag.	Phase	Mag.	Phase	Mag.	Phase
10	1.60	0	1.00	0	.731	0	.561	0
20	1.30	0	.60	0	.547	0	.376	0
30	1.10	0	.50	0	.444	0	.315	0
40	.95	0	.43	0	.387	0	.268	0
50	.90	0	.38	0	.362	0	.232	0
60	.85	0	.34	0	.356	0	.198	0
70	.80	0	.30	0	.360	0	.173	0
80	.70	0	.27	0	.329	0	.150	0
90	.50	0	.25	0	.237	0	.128	0
100	0	0	0	0	0	0	0	0

TABLE III. OSCILLATORY HYDRODYNAMIC COEFFICIENTS FOR $1/k = .500$

% Span	L_h		L_α		M_h		M_α	
	Mag.	Phase	Mag.	Phase	Mag.	Phase	Mag.	Phase
10	1.71	322°	1.55	269°	.675	8.5°	.644	311°
20	1.18	326°	1.01	271°	.525	13.3°	.454	314°
30	.925	331°	.910	274°	.436	17.3°	.400	316°
40	.770	336°	.810	276°	.375	20.9°	.351	317°
50	.715	339°	.725	278°	.336	23.5°	.316	318°
60	.695	343°	.650	280°	.315	25.8°	.284	319°
70	.665	345°	.590	282°	.299	28.1°	.261	320°
80	.615	347°	.530	284°	.270	30.2°	.244	321°
90	.515	348°	.480	286°	.213	31.3°	.226	321°
100	0	349°	0	288°	0	32.0°	0	321°

TABLE IV. OSCILLATORY HYDRODYNAMIC COEFFICIENTS FOR $1/k = .700$

%	L_h		L_α		M_h		M_α	
Span	Mag.	Phase	Mag.	Phase	Mag.	Phase	Mag.	Phase
10	1.84	308°	1.467	251°	.567	10.1°	.715	306°
20	1.28	311.5°	1.016	256°	.462	17.8°	.516	309°
30	.905	316°	.995	260°	.393	24.3°	.468	311.5°
40	.729	320.5°	.949	263.5°	.341	28.0°	.426	313°
50	.668	325°	.886	267°	.306	31.1°	.393	315°
60	.667	329°	.824	269°	.283	32.1°	.360	316°
70	.658	331°	.770	271°	.266	33.7°	.334	316°
80	.628	334°	.704	272.5°	.247	35.5°	.314	317°
90	.531	335°	.626	273°	.199	36.4°	.295	317°
100	0	336°	0	273°	0	37.0°	0	317°

TABLE V. OSCILLATORY HYDRODYNAMIC COEFFICIENTS FOR $1/k = .833$

%	L_h		L_α		M_h		M_α	
Span	Mag.	Phase	Mag.	Phase	Mag.	Phase	Mag.	Phase
10	2.210	300°	2.00	240°	.589	11.0°	.797	299°
20	1.515	304°	1.49	245.5°	.467	18.6°	.590	303°
30	1.065	308.5°	1.38	250°	.387	25.4°	.537	306°
40	.850	313°	1.27	254.5°	.333	29.2°	.496	309°
50	.765	318°	1.16	258.5°	.297	32.5°	.460	312°
60	.760	321.5°	1.06	261°	.274	33.7°	.427	313°
70	.740	324°	.975	263.5°	.258	35.6°	.397	315°
80	.695	327°	.890	265°	.243	38.1°	.373	316°
90	.570	329°	.800	265°	.197	39.4°	.347	317°
100	0	330°	0	265°	0	40.0°	0	317°

TABLE VI. OSCILLATORY HYDRODYNAMIC COEFFICIENTS FOR $1/k = .900$

%	L_h		L_α		M_h		M_α	
Span	Mag.	Phase	Mag.	Phase	Mag.	Phase	Mag.	Phase
10	2.459	296°	2.42	235°	.618	11.4°	.848	296°
20	2.676	301°	1.85	240°	.479	18.5°	.636	299°
30	1.186	305°	1.66	245°	.388	25.2°	.579	303°
40	.945	310°	1.49	250°	.332	29.1°	.537	307°
50	.843	315°	1.34	254°	.294	32.5°	.498	310°
60	.832	318°	1.21	257°	.272	33.9°	.465	312°
70	.802	321°	1.10	260°	.257	36.1°	.433	314°
80	.743	324°	1.00	261°	.243	39.2°	.405	316°
90	.598	326°	.906	262°	.198	40.8°	.375	317°
100	0	327°	0	262°	0	42.0°	0	317°

TABLE VII. OSCILLATORY HYDRODYNAMIC COEFFICIENTS FOR $1/k = 1.00$

%	L_h		L_α		M		M_α		
	Span	Mag.	Phase	Mag.	Phase	Mag.	Phase	Mag.	Phase
10		2.89	291.5°	3.22	228°	.675	12.0°	.937	289°
20		1.96	296°	2.53	233°	.503	18.0°	.717	293°
30		1.40	301°	2.18	238°	.395	24.4°	.651	298°
40		1.12	305°	1.90	243°	.333	28.3°	.606	303°
50		.987	310°	1.67	248°	.293	31.8°	.562	307°
60		.962	314°	1.47	251°	.272	33.7°	.526	310°
70		.913	317°	1.315	254°	.256	36.5°	.491	313°
80		.829	320°	1.19	256°	.244	40.5°	.459	316°
90		.649	322°	1.08	257°	.200	42.8°	.421	317°
100		0	323°	0	257°	0	45.0°	0	318°

TABLE VIII. OSCILLATORY HYDRODYNAMIC COEFFICIENTS FOR $1/k = 1.10$

%	L_h		L_α		M_h		M_α		
	Span	Mag.	Phase	Mag.	Phase	Mag.	Phase	Mag.	Phase
10		3.37	287°	4.20	221°	.739	12.5°	1.04	283°
20		2.28	292°	3.35	227°	.532	17.3°	.812	287°
30		1.67	296°	2.81	232°	.405	23.0°	.734	293°
40		1.32	301°	2.38	237°	.336	27.1°	.683	299°
50		1.15	306°	2.05	241.5°	.293	30.6°	.632	305°
60		1.11	310°	1.78	246°	.272	33.1°	.594	309°
70		1.04	313°	1.56	249°	.256	36.4°	.555	313°
80		.930	316°	1.39	252°	.246	41.5°	.517	316°
90		.712	319°	1.27	253°	.203	44.6°	.470	318°
100		0	320°	0	253°	0	47.0°	0	319°

TABLE IX. OSCILLATORY HYDRODYNAMIC COEFFICIENTS FOR $1/k = 1.25$

%	L_h		L_α		M_h		M_α		
	Span	Mag.	Phase	Mag.	Phase	Mag.	Phase	Mag.	Phase
10		4.14	279.5°	5.95	214.0°	.820	13.2°	1.22	274°
20		2.81	285.0°	4.80	219.5°	.570	16.1°	.978	279°
30		2.07	290.0°	3.92	224.5°	.420	21.1°	.878	286°
40		1.65	295.5°	3.24	230.0°	.340	25.2°	.813	294°
50		1.425	300.0°	2.72	234.0°	.291	28.8°	.750	301°
60		1.35	304.5°	2.30	239.0°	.270	31.9°	.707	307°
70		1.25	308.0°	1.97	243.0°	.254	35.9°	.661	313°
80		1.10	310.5°	1.73	246.0°	.245	42.5°	.614	317°
90		.830	313.5°	1.57	249.0°	.204	47.0°	.551	320°
100		0	315.0°	0	0	0	50.0°	0	322°

TABLE X. OSCILLATORY HYDRODYNAMIC COEFFICIENTS FOR $1/k = 1.67$

γ Span	L_h		L_α		M_h		M_α	
	Mag.	Phase	Mag.	Phase	Mag.	Phase	Mag.	Phase
10	5.97	253°	1.20	210°	.647	15.6°	1.90	263°
20	4.30	260°	.980	216°	.504	19.2°	1.61	269°
30	3.09	265.5°	.785	221°	.397	25.7°	1.42	278°
40	2.425	271.5°	.633	226°	.311	28.8°	1.28	287°
50	2.02	276.5°	.509	231°	.251	32.8°	1.17	296°
60	1.85	281.5°	.412	236°	.208	33.2°	1.09	303°
70	1.76	285°	.337	240°	.189	37.0°	1.02	310°
80	1.61	289°	.278	243°	.176	43.8°	.950	316°
90	1.31	291.5°	.235	246°	.169	51.8°	.842	320°
100	0	293.0°	0	248°	0	55.0°	0	321°

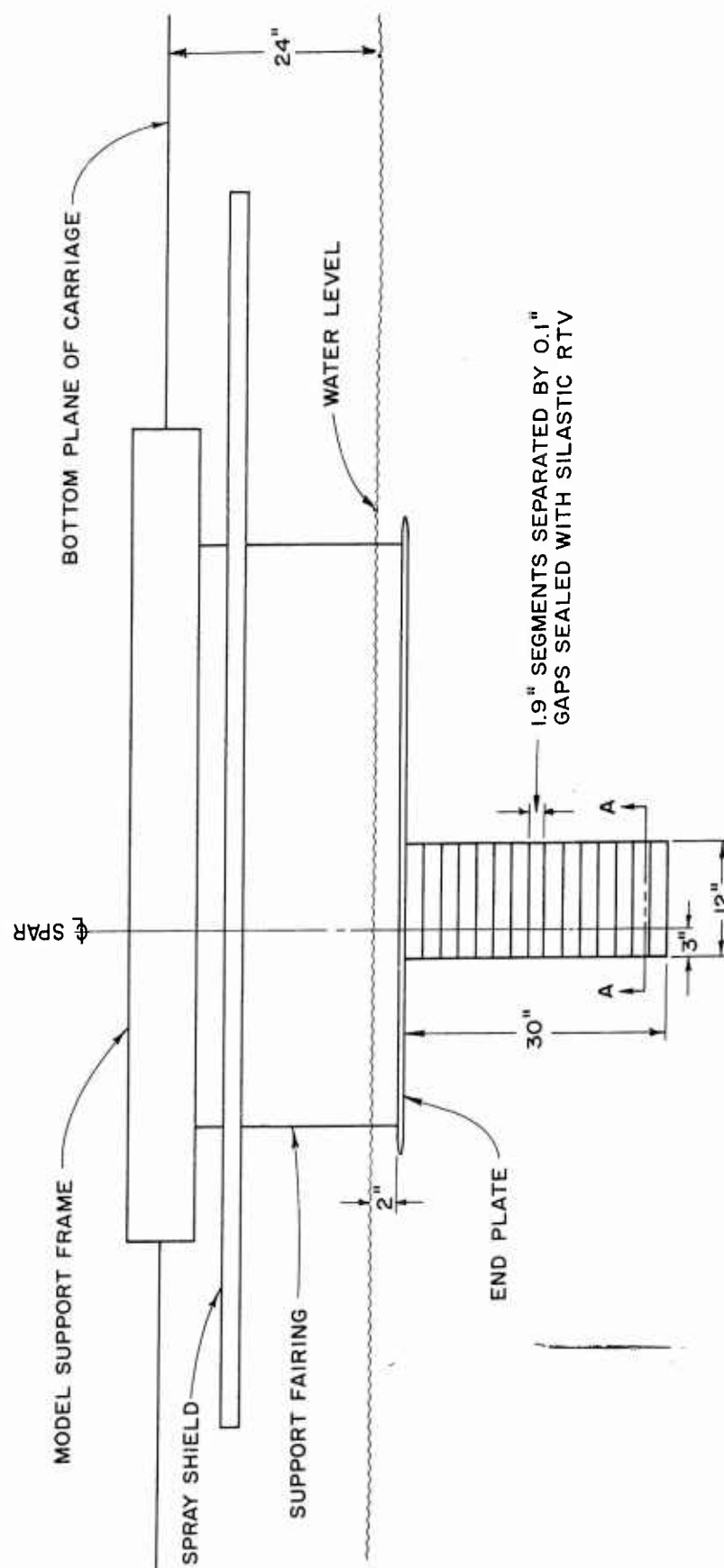
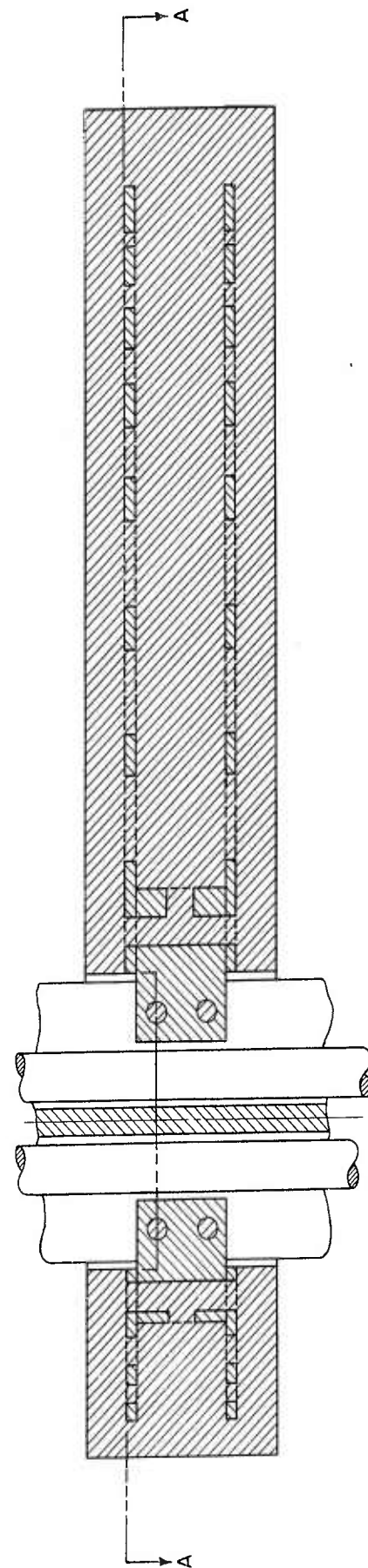
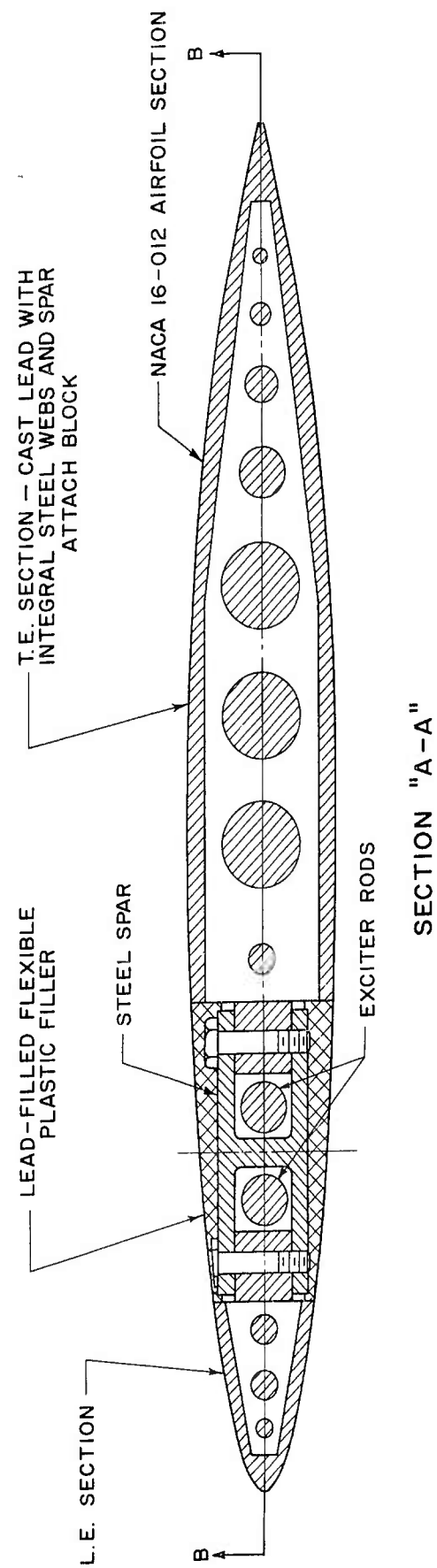


FIGURE 1 - SCHEMATIC LAYOUT OF FLUTTER MODEL AND SUSPENSION



SECTION "B-B"

FIGURE 2 - DETAILS OF FLUTTER MODEL CONSTRUCTION

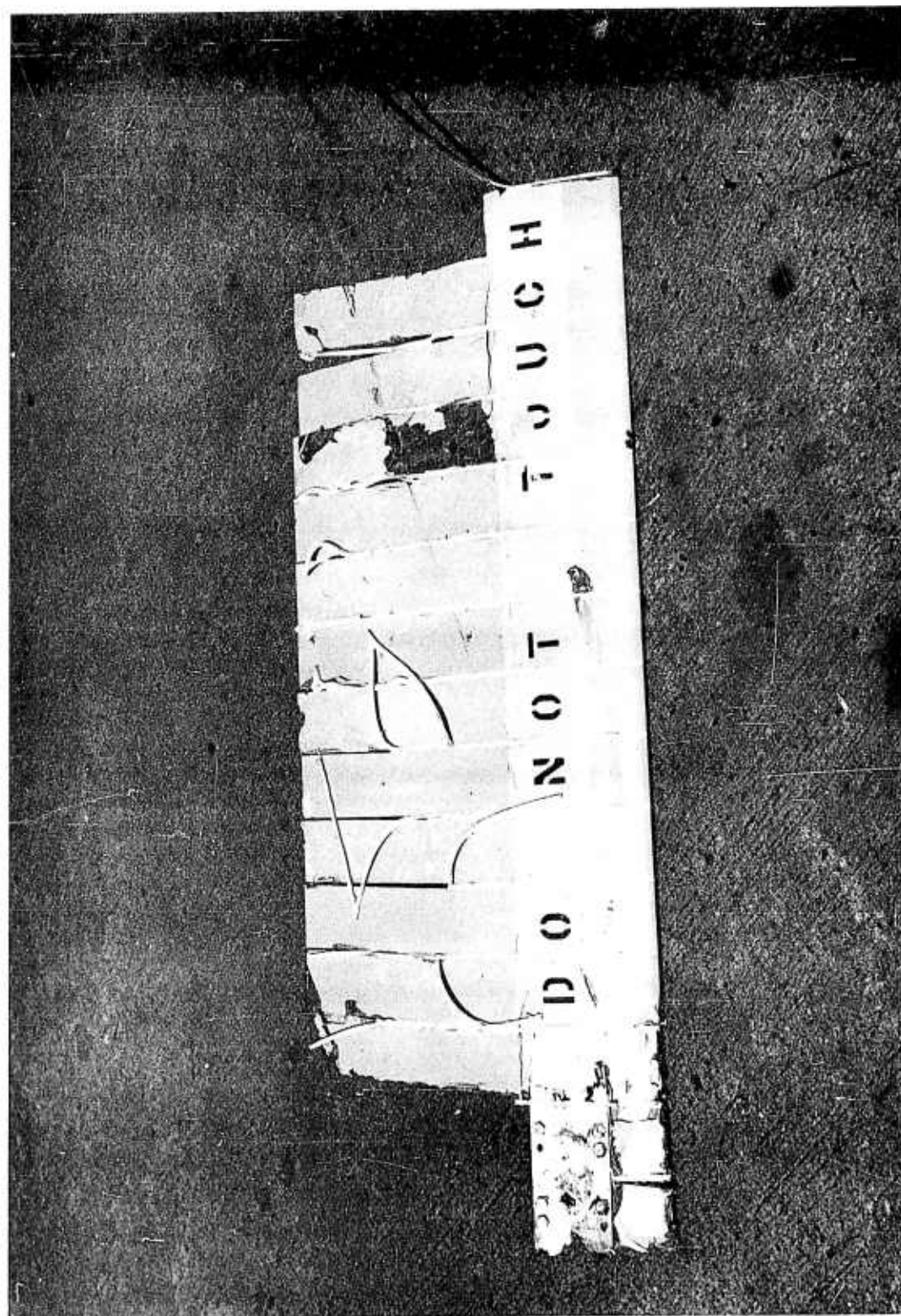


FIGURE 3 - FLUTTER MODEL FOLLOWING CATASTROPHIC FAILURE AT 48.1 KNOTS

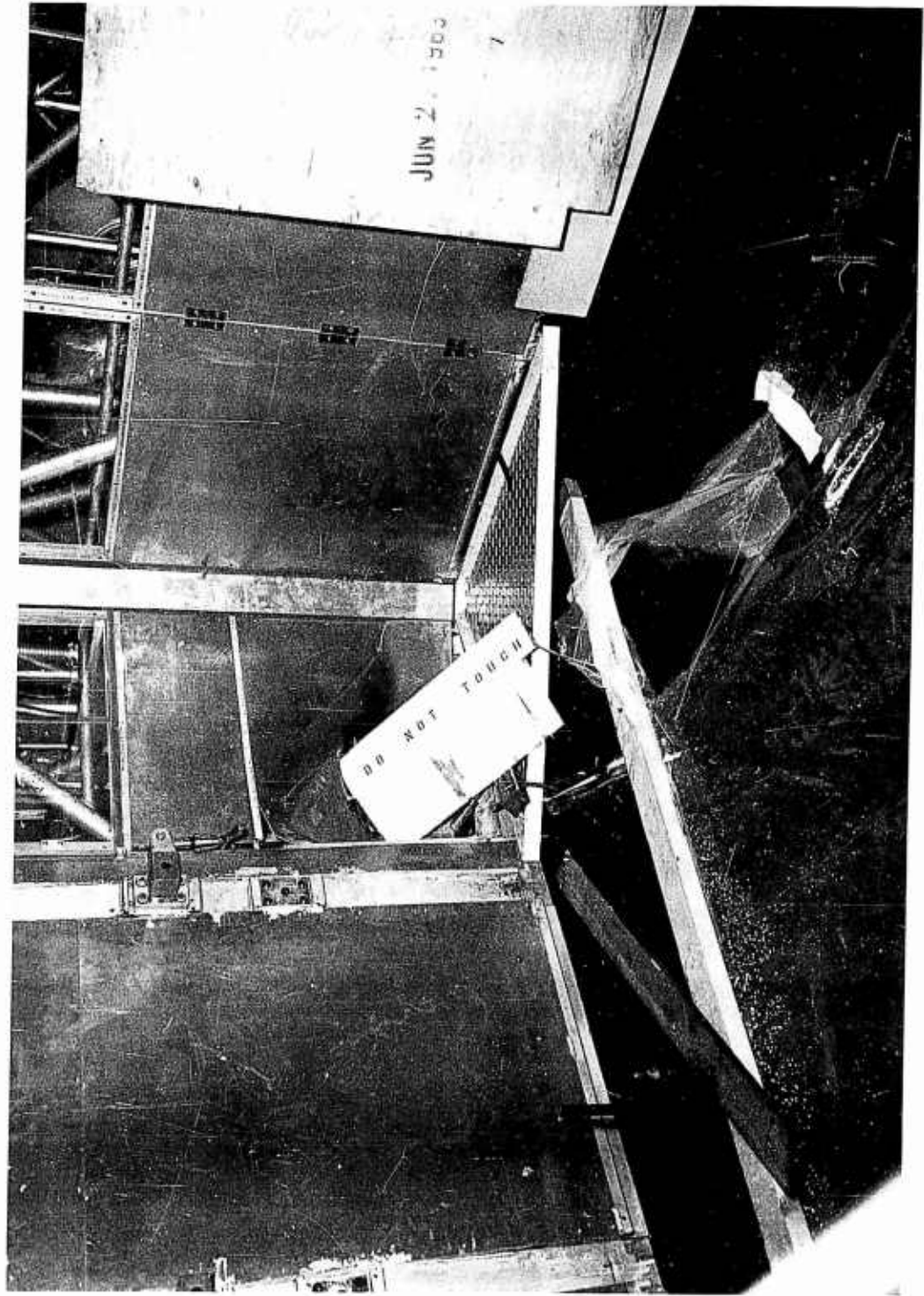


FIGURE 4 - FLUTTER MODEL IMPAIRED IN TOWING CARRIAGE
WALL FOLLOWING CATASTROPHIC FAILURE

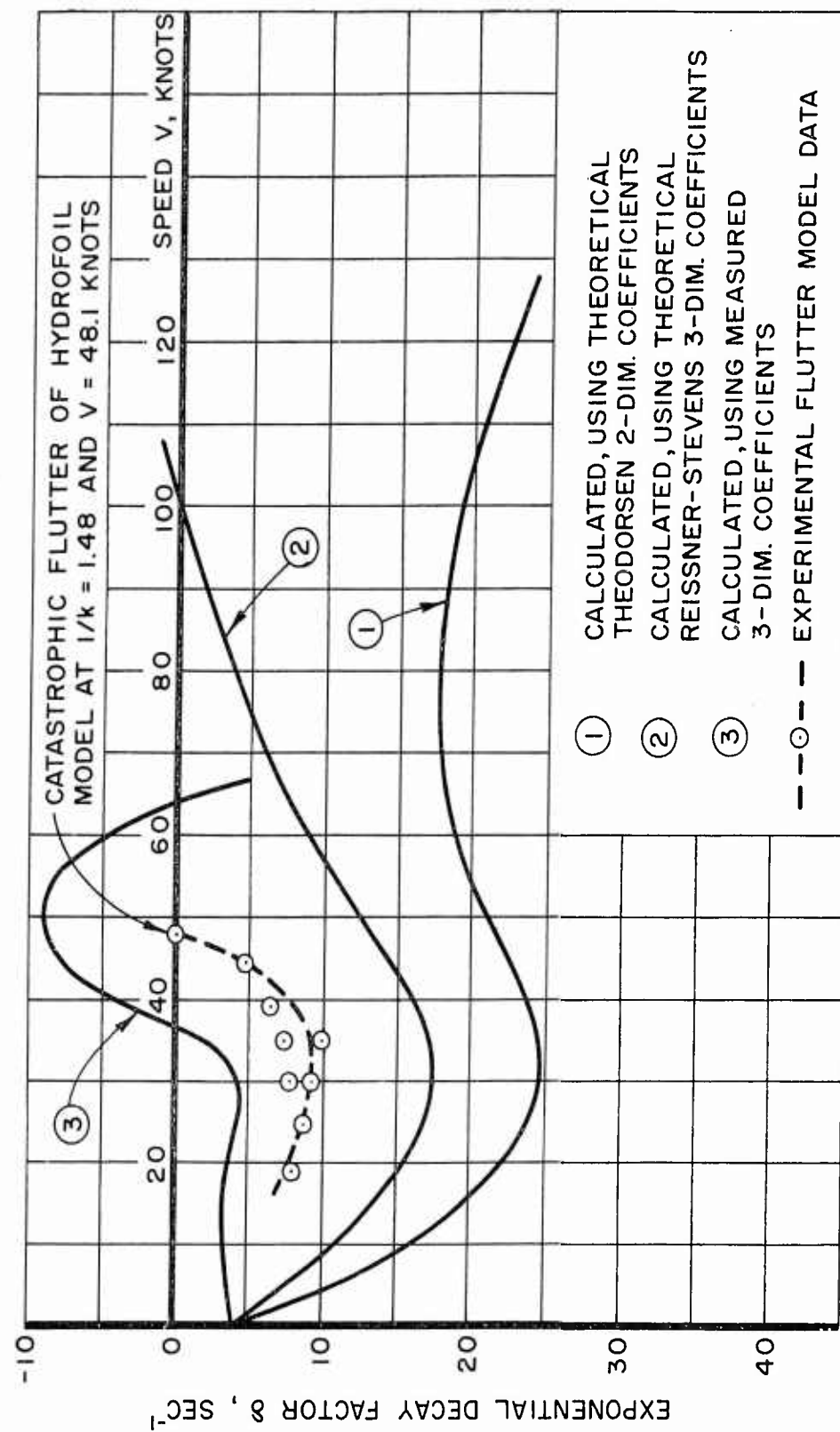


FIGURE 5 - FLUTTER MODEL EXPONENTIAL DECAY FACTOR VERSUS SPEED

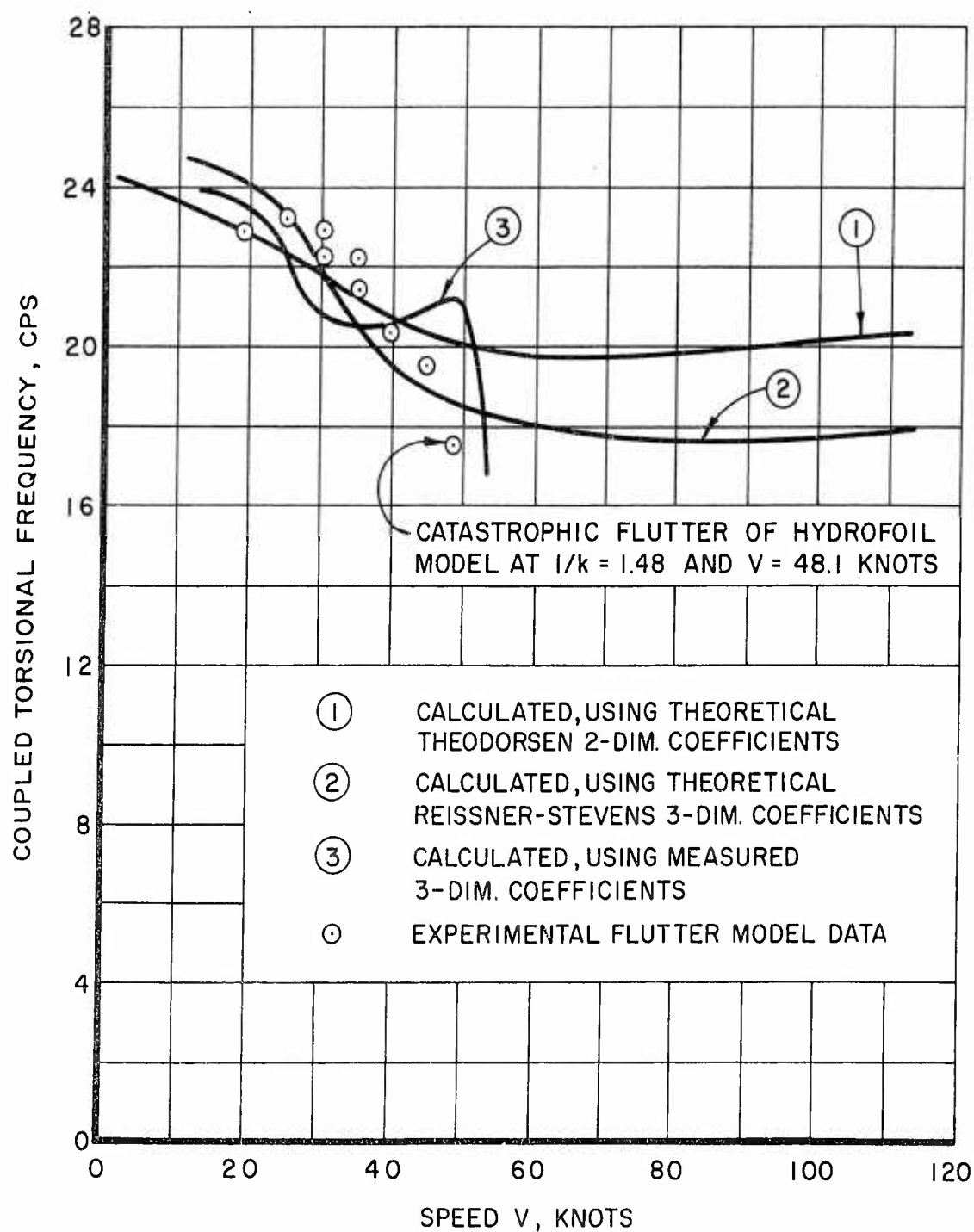


FIGURE 6 - COUPLED TORSIONAL FREQUENCY VERSUS SPEED

INITIAL DISTRIBUTION LIST
Contract Nonr-3335(00)

Chief, Bureau of Ships Department of the Navy Washington 25, D. C.	Commander Wright Air Development Division Aeronautical Systems Division (ASRMDD) Wright-Patterson Air Force Base, Ohio
(2) Attn: Preliminary Design (Code 420)	(1) Attn: Mr. W. Mykytow, Dynamics Branch
(3) Hull Design (Code 440)	Flight Dynamics Laboratory
(3) Technical Library (Code 210L)	
Commanding Officer and Director David Taylor Model Basin Washington 7, D. C.	Boeing Airplane Company Seattle Division Seattle, Washington
(60) Attn: Contract Res. Adm. (Code 513)	(1) Attn: Mr. M. J. Turner
Chief of Naval Research Fluid Dynamics Branch (Code 438) Department of the Navy	California Institute of Technology Pasadena, California
(2) Washington 25, D. C.	(1) Attn: Dr. M. S. Plesset
Chief, Bureau of Naval Weapons Dynamics Section (Code RAAD-222)	(1) Dr. T. Y. Wu
(1) Washington 25, D. C.	(1) Dr. A. J. Acosta
Commander U. S. Naval Ordnance Laboratory	Convair Post Office Box 1950 San Diego 12, California
(1) White Oak, Maryland	(1) Attn: Mr. R. Peller
Commander U. S. Naval Ordnance Test Station	Systems Dynamics Group
(1) China Lake, California	(1) Mr. H. T. Brooke
Officer-in-charge, Pasadena Annex U. S. Naval Ordnance Test Station Oceanic Research (Code P-508) 3202 E. Foothill Blvd.	Hydrodynamics Group
(2) Pasadena 8, California	Cornell Aeronautical Laboratory 4455 Genesee Street Buffalo, New York
National Bureau of Standards Washington 25, D. C.	(1) Attn: Dr. I. Statler
(1) Attn: Dr. G. B. Schubauer, Chief	(1) Mr. R. White
Fluid Mechanics Section	Director, Davidson Laboratory Stevens Institute of Technology Hoboken, New Jersey
(1) Dr. J. M. Franklin	(1) Attn: Mr. C. J. Henry
Consultant	(1) Mr. S. Tsakonas
Director Langley Research Center Langley Field, Virginia	Electric Boat Division General Dynamics Corporation Groton, Connecticut
(1) Attn: Mr. I. E. Garrick	(1) Attn: Mr. Robert McCandliss
(1) Mr. D. J. Marten	General Applied Sciences Laboratories, Inc. Merrick and Stewart Avenues Westbury, Long Island, New York
Mr. R. P. Godwin, Acting Chief Office of Research & Development Maritime Administration 441 G. Street, Northwest	(1) Attn: Dr. F. Lane
(1) Washington 25, D. C.	Gibbs and Cox, Incorporated 21 West Street New York, New York
Commander Armed Services Tech. Inf. Agency Attention: TIPDR Arlington Hall Station	Grumman Aircraft Engineering Corporation Bethpage, Long Island, New York
(10) Arlington 12, Virginia	(1) Attn: Mr. E. Baird
Commander Air Research & Development Command Attention: Mechanics Branch Air Force Office of Scientific Research 14th and Constitution	(1) Mr. C. Squires
(1) Washington 25, D. C.	Grumman Aircraft Engineering Corporation Dynamic Developments Division Babylon, New York
	President Hydronautics, Incorporated Pindell School Road Howard County
	(2) Laurel, Maryland

INITIAL DISTRIBUTION LIST

Contract Nonr-3335(00)

(Continued)

Lockheed Aircraft Corporation
Missiles and Space Division
Palo Alto, California
(1) Attn: Mr. R. W. Kermeen

Massachusetts Institute of Technology
Fluid Dynamics Research Laboratory
Cambridge 39, Massachusetts
(1) Attn: Prof. H. Ashley
(1) Prof. M. Landahl
(1) Prof. J. Dugundji

Midwest Research Institute
425 Volker Blvd.
Kansas City 10, Missouri
(1) Attn: Mr. Zeydel

Pennsylvania State University
Ordnance Research Laboratory
University Park, Pennsylvania
(1) Attn: Dr. M. Sevik

Southwest Research Institute
Dept. of Mechanical Sciences
8500 Culebra Road
San Antonio 6, Texas
(1) Attn: Dr. H. N. Abramson, Director
(1) Mr. G. E. Ransleben, Jr.
(1) Editor, Applied Mechanics Reviews

Stanford University
Department of Mathematics
Stanford, California
(1) Attn: Dr. Robert Street
(1) Dr. E. Y. Hsu

State University of Iowa
Iowa Institute of Hydraulic Research
Iowa City, Iowa
(1) Attn: Prof. L. Landweber

Technical Research Group, Incorporated
2 Aerial Way
(2) Syosset, Long Island, New York

The Rand Corporation
1700 Main Street
Santa Monica, California
(1) Attn: Dr. B. Parkin

University of California
Department of Engineering
Institute of Engineering Research
Berkeley, California
(1) Attn: Dr. J. V. Wehausen

University of California
Department of Naval Architecture
Berkeley, California
(1) Attn: Prof. H. A. Schade, Head

University of Minnesota
St. Anthony Falls Hydraulic Lab.
Minneapolis, Minnesota
(1) Attn: Prof. B. Silberman
(1) Mr. J. N. Wetzel

Oceanics, Incorporated
Technical Industrial Park
Plainview, Long Island, New York
(1) Attn: Dr. P. Kaplan

Department of Mechanical Engineering
Aeronautics Laboratory
Illinois Institute of Technology
Technology Center
Chicago 16, Illinois
(1) Attn: Dr. I. Michelson

Vidya
1450 Page Mill Road
Palo Alto, California
(1) Attn: Dr. J. Nielson